Dealkylation of Alkylbenzenes: A Significant Pathway in the Toluene, *o*-, *m*-, *p*-Xylene + OH Reaction

Jun Noda,[†,‡,§] Rainer Volkamer,*[,†,∥,⊥] and Mario J. Molina[†,∥]

Earth, Atmospheric and Planetary Sciences, Massachusetts Institute of Technology, Cambridge, Massachusetts 02139, Chemistry and Biochemistry, University of California, San Diego, La Jolla, California 92093, and Atmospheric Science, Department of Chemistry, University of Gothenburg, S-41296 Gothenburg, Sweden

Received: February 19, 2009; Revised Manuscript Received: June 29, 2009

The OH-radical initiated oxidation of a series of monocyclic aromatic hydrocarbons (benzene, toluene, *o*-, *m*-, and *p*-xylene) in the presence of oxygen and NO_x was investigated in a flowtube coupled with a chemical ionization mass spectrometer (CIMS). OH-radical addition to the aromatic ring — the major reaction pathway — has previously been shown to have a particular sensitivity to experimental conditions. This is the first flowtube study that demonstrates the atmospheric relevance of product yields from the OH-addition channel on the millisecond time scale (35−75 ms); the phenol yield from benzene and cresol yields from toluene are found to be 51.0 ± 4.3% and 17.7 ± 2.1%, in excellent agreement with previous studies under close to atmospheric conditions. We further report unambiguous experimental evidence that dealkylation is a novel and significant pathway for toluene and *o*-, *m*-, and *p*-xylene oxidation. At 150 Torr of O_2 partial pressure, toluene is found to dealkylate with a yield of 5.4 ± 1.2% phenol; similarly, *m*-, *o*-, and *p*-xylene dealkylate with yields of 11.2 ± 3.8%, 4.5 ± 3.2%, and 4.3 ± 3.1% cresol, respectively. A dealkylation mechanism via OH-addition in the ipso position is feasible ($\Delta H = -9$ kcal/mol for phenol formation from toluene) but does not lend itself easily to explain the significant isomer effect observed among xylenes; instead an alternative mechanism is presented that can explain this isomer effect and forms phenol and likely epoxide type products with identical *m*/*z* (indistinguishable in our CIMS analysis) via a carbene-type intermediate. Dealkylation adds to the atmospheric production of phenol- and likely epoxide-type products, with aldehydes as expected co-products, and helps improve the carbon balance in the initial stages of aromatic oxidation.

Introduction

Urban air quality is becoming an increasingly important issue as more than half of the global population now resides in urban areas.[1] It is important to characterize the atmospheric degradation pathways of volatile organic compounds (VOC) such as benzene, toluene, and other alkyl benzenes because aromatics account for 20−40% of the VOC in urban areas.[2,3] Aromatics are major contributors to photochemical smog, due to their high reactivities toward OH-radicals. In the presence of nitrogen oxides (NO_x) and sunlight their oxidation contributes to the formation of ozone, other oxidants, and particulate matter.[4] Laboratory studies find total carbon yields (sum of gas- and aerosol-phase products) for toluene, *m*-xylene, and *p*-xylene, the most widely studied aromatic compounds, to be on the order of 50−70%; thus about one-third to one-half of the carbon in form of oxidation products from aromatics is presently unidentified.[5,6] Even for toluene, the most well-studied aromatic compound, the sum of molar branching ratios for the first generation oxidation products does not add up to unity. It falls short by some 10%, and this gap appears to be significant within reduced measurement uncertainties,[7] indicating that further oxidation pathways remain to be identified in the early stages of aromatic oxidation. Our incomplete knowledge of the oxidation pathways of aromatics leads to uncertain predictions of ozone, secondary organic aerosol (SOA) formation, and the oxidative capacity in urban air.[8,9]

TABLE 1: Phenol Yields from the Benzene + OH System

experiment OH + benzene	% yield (phenol)	experimental conditions: time scale	experimental conditions: NO_x (ppm)
this work	51.0 ± 4.3	0.035−0.09 s	0.01−0.1 NO_x
Bjergbakke et al.[49]	10 ± 5[a]	0.25−2.5 s	no NO_x
Berndt et al.[16]	28 ± 7[a]	0.37−2 s	no NO_x
Berndt and Boge[17]	25 ± 5	0.26−0.42 s	3−10 NO_x
Atkinson et al.[28]	23.6 ± 4.4	ca. 10 min	1−20 NO_2
Volkamer et al.[14]	61.2 ± 7.0	5 min−2 h	no NO_x (<0.002)
Volkamer et al.[14]	53.1 ± 6.6	5 min−2 h	0.02−0.1 NO_x
Volkamer et al.[14]	25.2 ± 4.0	5 min−2 h	2 NO_x
Klotz et al.[11]	25 ± 4.0	5 min−1 h	1.4 NO_2
Klotz et al.[11]	8 ± 3.0	5 min−1 h	14 NO
Berndt and Böge[15]	60 ± 10	ca. 10 min	no or <0.06 NO_x

[a] Values re-evaluated as discussed in ref 14.

The OH-radical addition to the aromatic ring is the dominant reaction pathway for aromatic oxidation.[4,10] It is now established that the products formed from the OH-addition channel exhibit a particular sensitivity to experimental conditions, i.e., NO_x concentrations for benzene,[11,12] and *p*-xylene,[12,13] and HO_x concentrations as is further discussed in Volkamer et al..[14] This is illustrated in Table 1 for the phenol yield from the benzene + OH reaction: while there is good agreement among studies

* Corresponding author, rainer.volkamer@colorado.edu.
† Massachusetts Institute of Technology.
‡ University of Gothenburg.
§ Present address: Department of Health and Environmental Sciences, Rakuno Gakuen University, Ebetsu, Hokkaido, 069-8501, Japan.
∥ University of California, San Diego.
⊥ Present address: Department of Chemistry & Biochemistry and CIRES, University of Colorado at Boulder, Boulder, Colorado 80309-0215.

10.1021/jp901529k CCC: $40.75
Published on Web 08/06/2009

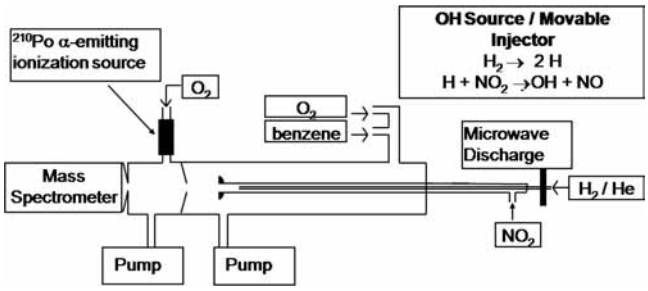

Figure 1. Sketch of the experimental setup: a flowtube with movable injector coupled to a chemical ionization mass spectrometer (CIMS).

that were conducted under atmospherically relevant conditions, i.e., 53.1 ± 6.6%[14] and 60 ± 10%,[15] significant differences are observed among flowtube studies, which show systematically lower yields.[16,17] Flowtube studies achieve reduction in the oxidation time scales by increasing the levels of oxidants by several orders of magnitude compared to atmospheric conditions; the scatter among those studies is as large as a factor of 5 (see Table 1). In contrast, product yields from the OH-abstraction channel for toluene agree to within a few percent between simulation chamber and flowtube studies.[6,18,19] These particular sensitivities of the OH-addition channel to experimental conditions require active measures to be taken to demonstrate the atmospheric relevance of results. The formation of phenol-type products makes for a particularly good sample system to demonstrate the atmospheric relevance, (1) as phenols are major oxidation products from the OH-addition pathway of aromatic oxidation, (2) for benzene and toluene the respective yields of phenol and cresols have been determined by independent research groups and are in good agreement under atmospherically relevant conditions,[6,14,15,18] and (3) phenol-type products are deemed the coproduct of so-called "prompt" HO_2 that is observed in OH cycling experiments on a time scale of milliseconds. However, a direct and quantitative confirmation of phenol-type products as quantitative coproducts of "prompt HO_2" (HO_2 formed without any delay from the reaction of RO_x with NO) is currently missing. It is further presently not clear whether the difference in phenol yields from flowtube reactions and smog chambers is caused by different experiment time scales or is due to competing reaction pathways under different experimental conditions.

Experimental Methods

Flowtube. All experiments were carried out in a flowtube (FT) system which was coupled to a chemical ionization mass spectrometer (CIMS). At the heart of the system was a 120 cm long and 2.54 cm inner diameter FT equipped with a movable injector as is shown in Figure 1. The injector has two functions, introducing OH radicals to the system and varying the reaction time in the FT. Reaction times were varied between 35 and 75 ms, and the typical reaction time setup was ca. 50 ms. The FT pressure was maintained at 154 ± 4 Torr for all experiments. The chemical ionization (CI) region was differentially pumped to a pressure of 18.5 ± 1 Torr by a separate rotary vane vacuum pump. Pressures inside the FT and the CI regions were continuously monitored by Baratron-MKS pressure gauges (Andover, MA) to maintain constant pressure by manual adjustment of needle valves. All inner surfaces of the FT and injector components were coated with Halocarbon-wax (River Edge, NJ) to minimize wall loss of OH-radicals and other compounds. The quadrupole mass spectrometer pressure was maintained at pressures of ca. 1×10^{-5} Torr by turbo pumps backed by a rotary vane pump. A flow of 50 SLPM oxygen/nitrogen gas mixture (10−98%) was used as carrier gas under turbulent plug-flow conditions ($Re > 3000$) in the FT to additionally decrease the OH-radical loss to the FT walls and increase the OH lifetime in the FT.[20] Control experiments were conducted to characterize the OH-radical wall loss rate and the loss-rate in the background carrier gas, which were in total about 2×10^{-3} s^{-1}.

OH radicals were generated by passing H_2 in He (>99.999%) through an oxygen trap and a liquid nitrogen cooled silica gel trap before introduction to a microwave discharge (MWD) to produce H-atoms that were subsequently titrated by addition of NO_2 inside the movable injector by reactions 1 and 2:

$$H_2 + MWD \rightarrow 2H \quad (1)$$

$$H + NO_2 \rightarrow OH + NO \quad (2)$$

The OH radical concentrations inside the FT were typically about 2×10^{11} molecules cm^{-3}. The number of OH radicals that reacted in a given experiment was quantified by the relative decrease of an OH tracer substance, e.g,. 2,4,6-trimethylphenol (2,4,6-TMP) which was added in trace amounts together with the aromatic hydrocarbon under examination. Further details of this tracer method are described in the following Evaluation section. The aromatic compounds and the tracer gas were added directly upstream of the FT with a 1 SLPM flow of carrier gas that was nitrogen or helium.

Chemical Ionization Mass Spectrometry. An Extrel/ABB quadrupole CIMS (Pittsburgh, PA) was employed to monitor phenol-type compounds (tracer and products) in their protonated forms by using a series of protonated water clusters as a soft ionization source ($H^+(H_2O)_n$ with $n = 2$ and 3 as dominant water cluster ions). The distributions of the four lowest-mass water cluster ion signals ($m/z = 19$, 37, 55, and 73 and $n = 1$, 2, 3, and 4, respectively) were monitored during all calibration runs to identify possible cluster ion distribution effects in addition to frequent calibration of the sensitivity toward phenol-type compounds, as described in the following section Gas Calibration and CIMS Sensitivity. The water clusters were generated from oxygen (<99.8%) containing a trace amount of water that was flowed through a ^{210}Po source Nuclecel In-Lines P-2031 (Grand Island, NY) at 3 SLPM. The CI region was separated from the main FT by a 1 mm pinhole. Only about 1 SLPM of the FT gas flow entered the CI region and participated in the ionization process. Phenol type products were monitored at their characteristic mass-to-charge ratio (m/z) in their protonated form $(R + H)^+$.

Gas Calibration and CIMS Sensitivity. The aromatic hydrocarbons and the tracer compound were introduced into the flow tube using pure helium or nitrogen (<99.999%) as a carrier gas. Heating tape kept all tubing for the aromatics compounds at ca. 60 °C to minimize wall adsorption. A known pressure of each hydrocarbon was mixed with clean helium gas in a glass bulb, and each gas mixture was calibrated using a UV spectrometer, Varian Cary 5E (Palo Alto, CA) before and after each set of experimental runs. The CIMS signal from the phenol-type compounds was calibrated by flowing known volumes of authentic phenol samples using two approaches: (1) mixtures of phenol prepared in helium in a glass bulb, and (2) phenol grains added to a fritted bubbler. In method (1), the bulb was allowed to sit for a few days to equilibrate at room

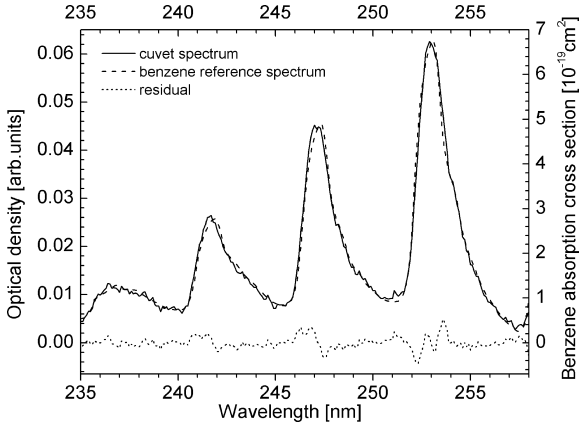

Figure 2. Solid line indicates UV spectrum of benzene observed in a cuvet filled with 28.2 Torr of a 1.04% dilute benzene/helium gas mixture. Comparison with a dashed line scaled literature spectrum of benzene provides calibration of the gas mixture with a precision of 2σ, 5%. The difference between the spectra is shown as the short dashed line.

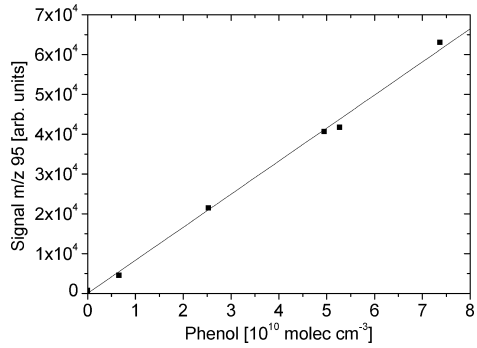

Figure 3. Calibration of the CIMS response to phenol using transfer of protonated water clusters $H^+(H_2O)_n$ as ionizing reaction.

temperature. Known volumes were extracted from the bulb into a cuvette, and a UV spectrum was recorded using the UV spectrometer. The literature cross section of phenol was adjusted to match the spectral resolution of the UV spectrometer and was then scaled using nonlinear least-squares fitting routines to determine the mixing ratio inside the bulb.[21,22] Figure 2 shows an example of the UV spectra that were recorded periodically; diluted mixtures of phenol/He were found stable within 5% over periods of weeks after conditioning. In method (2), a few grains of phenol were added to a fritted bubbler and the vapor concentration in a known volume flow of He was calculated based on the known vapor pressure of phenol.[23] Both approaches to calibrate the phenol agreed to within 10%. Figure 3 illustrates the response of the CIMS to phenol, which was linear to within the measurement precision of a few percent. This setup provided excellent sensitivity for phenol-type compounds, with detections limits of the order of 5×10^7 molecules cm^{-3} (or 10 pptv; 1 pptv $= 10^{-12}$). The CIMS sensitivity toward different isomers of cresol and dimethylphenol was tested using similar procedures; the tests indicated similar sensitivity within the error limits and no isomer effects were observed for the tested compounds. The purities and sources of all the authentic samples used were benzene (>99%, Aldrich), *o*-, *m*-, and *p*-xylenes (>99%, Aldrich), toluene (>99%, Aldrich), phenol (>99%, Alfa Lancaster), 2,4-benzaldehyde (>99%, Alfa Aesar), 3,4-dimethylbenzaldehyde (>99%, Lancaster), 3-ethyltoluene (>98%, TCI America), 2,5-dimethylphenol (100%, Alfa Aesar), 3,4-dimethylphenol (>98%, Lancaster), *o*-cresol (≥99.5%, Fluka), *m*-cresol (≥99%, Fluka). Freeze−pump−thaw cycles were repeated several times

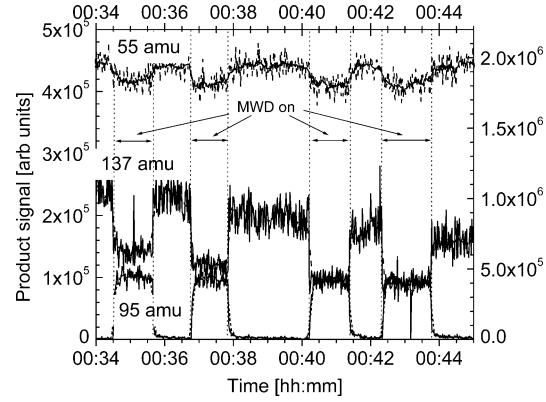

Figure 4. Time series of an experiment for determining the phenol yield from the benzene + OH reaction. Detected signals are parent ion m/z 55 $H^+(H_2O)_3$, tracer ion 2,4,6-TMP m/z 137 H^+(TMP), and m/z 95 H^+ (phenol). Gray shaded areas indicate times when the microwave discharge is turned on.

for each of the investigated compounds to eliminate dissolved gases before preparation of gas mixtures with helium. All gases were delivered via flowmeters Tylon General, FM-360 series (Torrance, CA) with accuracy of <±2%, which were periodically calibrated by a wet bubble flow calibration system, Gilibrator-2 (Clearwater, FL) with accuracy of <±3%. All carrier gases and other sweep gases to transfer gases into the FT and in the CI regions were obtained from Airgas Co., oxygen (>99.8%), nitrogen (>99.998%), and helium (>99.998%); the gas used for H_2 was helium (>99.999%).

Evaluation. Accounting for the regeneration of OH radicals inside the flow system requires the addition of a tracer substance. It is necessary to quantify this regeneration in order to accurately determine the amount of reacted parent aromatic compound. Numerical models of radical cycling do not give sufficient precision to be used for quantification due to considerable uncertainty in aromatic oxidation. Figure 4 illustrates an experiment time series for the determination of phenol yield from the benzene + OH reaction. The differences in signal intensities were measured and used for the evaluation below. It is reasonable to assume that the changes in signals were only due to OH radical reactions since the tracer signal depended only on the presence of OH radicals and recovered to the initial signal in the absence of OH radicals. The amount of reacted OH radicals was found according to eq 3.

$$[\mathrm{OH}]t = \frac{\ln\left(\frac{[2,4,6\text{-TMP}]_{\mathrm{ON}}}{[2,4,6\text{-TMP}]_{\mathrm{OFF}}}\right)}{k_{\mathrm{OH}}} \qquad (3)$$

where the tracer compound signal denoted as $[2,4,6\text{-TMP}]_{\mathrm{on/off}}$ at times when the microwave discharge (MWD) was turned "ON" and "OFF", k_{OH} ($1.31 \pm 0.15 \times 10^{-10}$ cm^3 molecules^{-1} s^{-1}) is the reaction rate constant of 2,4,6-TMP with OH radicals,[24] t is the reaction time, and $[\mathrm{OH}]t$ is the OH concentration integrated over time. The approximate concentrations of the tracer were ca. 9×10^9 and 5×10^9 molecules cm^{-3} without and with presence of OH radicals, respectively. Absolute calibration or measurement of 2,4,6-TMP is not necessary to evaluate this equation because only relative signals ("ON" vs "OFF") enter eq 3. Similarly, wall losses are already accounted for in the $[2,4,6\text{-TMP}]_{\mathrm{ON}}$ and $[2,4,6\text{-TMP}]_{\mathrm{OFF}}$ signals.

The phenol yield (Y_{phenol}) from benzene was calculated using eq 4

$$Y_{\text{Phenol}} = \frac{([\text{phenol}]_{\text{ON}} - [\text{phenol}]_{\text{OFF}})f_C}{[\text{benzene}]k_{\text{OH,benzene}}[\text{OH}]t} \quad (4)$$

where values in brackets correspond to calibrated concentrations of the respective species when the MWD was turned "ON" and "OFF", $k_{\text{OH,benzene}}$ (1.23×10^{-12} cm^3 molecules^{-1} s^{-1}) is the reaction rate constant of benzene with OH radicals,[13] and $f_C = 1 + (k_{\text{OH,phenol}}[\text{OH}]tf_{\text{profile}})$ accounts for phenol loss due to OH-radical reaction. $k_{\text{OH,phenol}}$ ($2.7 \pm 0.7 \times 10^{-11}$ cm^3 molecules^{-1} s^{-1}) is the reaction rate constant of phenol with OH radicals,[4] [OH]t is determined from the tracer, and the factor f_{profile} ranges between 0 and 1 and accounts for the fact that the concentration of phenol is increasing along the length of the flowtube. The OH profile along the FT was determined by means of numerical simulations for which the Master Chemical Mechanism[25] was initialized with typical initial concentrations; f_{profile} has a value of 0.5 for experiments with the injector close to the CI region, and 0.60 and 0.75 for middle and remote injector positions. Use of the tracer method to determine [OH]t eliminates the requirement of accurately known mixing processes at the injector outlet and accounts for regeneration of OH via the reaction of HO_2 with NO or RO_2. Typical values for f_C ranged from 1.03 to 1.13; uncertainties in determining f_C add a very small error to the final yield numbers. The uncertainty in Y_{phenol} is determined primarily by the accuracy of the concentrations of benzene which is limited by knowledge of the differential cross section (7.2% error), flow calibration (1% error), the phenol calibration (7% error), and the accuracy of the variables entering eq 3 (8% error), giving an overall uncertainty of the phenol yields of about 13%.

Results and Discussion

Prior to the series of experiments using different aromatic compounds, benzene and toluene were investigated extensively to optimize and characterize the FT system. Benzene is the most susceptible to interfering reactions with NO_x and HO_x and it is the molecule for which the overall loss rate from the initial equilibrium of the aromatic OH adduct and the aromatic OH peroxy radical is slowest,[26,27] also making it most vulnerable to other possible interfering reactions. Further, the phenol yields from benzene and the cresol yields from toluene are now considered as well established. The experimental value for the phenol yield from benzene was independently determined by three teams of researchers using four different experimental setups at EUPHORE, NIES, FORD, and IFU using the same set of spectroscopic parameters for calibration purposes as were used in this study,[11,12,15] and all of which yielded consistent results. For toluene, two teams of researchers have found consistent results.[6,18]

Benzene System: Phenol Yield. The phenol yields were measured as a function of the following parameters: (1) OH generation, which was varied by (a) changing the concentration of H_2 via the MWD, (b) the addition of parts per million levels of oxygen via the MWD, (c) the efficiency of H-atom titration to OH radicals by adding variable concentrations of NO_2 to the OH-source region inside the injector, and (d) the addition of trace amounts of NO to the OH-source region inside the injector; (2) reaction time of OH with benzene inside the FT which was varied by changing the injector position, (3) benzene concentration, (4) the O_2/N_2 mixing ratio in the FT bath gas, and (5) NO in the FT, which was added in concentrations of up to about 10^{13} molecules cm^{-3}.

In this study the phenol yield decreased at shorter OH lifetimes and when high concentrations of HO_2 radicals were present in the FT. It was found to be insensitive to parts per million levels of oxygen added to the helium carrier gas of the MWD used to generate OH radicals, in the presence of low variable NO_x levels. Phenol yields increased with experiments that used longer lifetimes of OH radicals and when trace amounts of NO were added during the generation of OH radicals. The average phenol yield (i.e., 51.0 ± 4.3%) was observed at an overall OH lifetime of 650 ms, or about 7×10^{11} and 1×10^{10} molecules cm^{-3} of benzene and 2,4,6-TMP, respectively. Figures 5, 6, and 7 show the plots of the phenol yield against some of the parameters to demonstrate the stability of the setup under different injector positions (Figure 5, reaction times varied from 35 to 75 ms); results did not depend on the fraction of OH radicals that reacted with benzene or the tracer (Figure 6, benzene concentrations varied from 8×10^{11} to 4×10^{13} molecules cm^{-3}), or the O_2 concentration (Figure 7,O_2/N_2 mixing ratio of the FT bath gas varied from 10 to 98%). The phenol yields were found to be approximately constant over a wide range of experimental conditions.

Table 1 gives the phenol yields from this work and previously reported literature values. The phenol yield presented here, 51.0 ± 4.3%, agrees within the error limits with that determined in a previous smog chamber study, 53.1 ± 6.6%, under close to

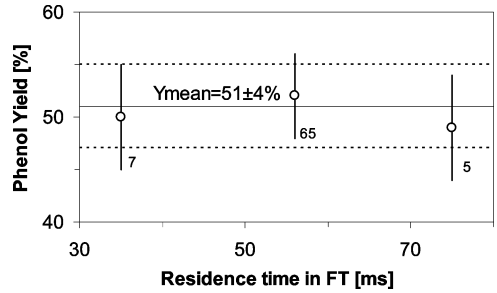

Figure 5. Phenol yields as a function of the OH radical and benzene reaction time. The numbers of individual FT experiments are indicated for each data point; error bars indicate the combination of variability between experiments and experimental uncertainty.

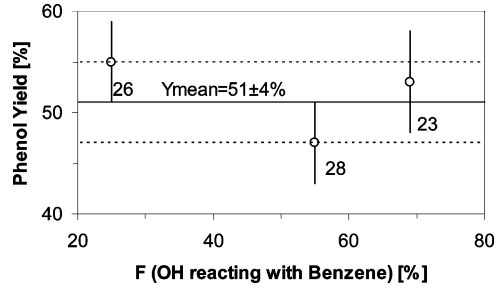

Figure 6. Phenol yields from the benzene + OH reaction did not depend on the fraction of OH reacting with benzene (1-F is the faction reacting with the tracer).

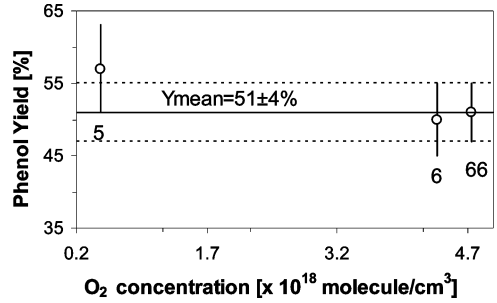

Figure 7. Phenol yields from benzene + OH as a function of the O_2 concentration in the FT (all experiments use 154 Torr total pressure and variable O_2/N_2 gas mixtures).

atmospheric conditions.[14] The most recent yield determined by Berndt and Böge (60 ± 10%)[15] also agrees well with the smog chamber study[14] and this study. Differences from results by Atkinson et al.[28] can be explained by deviations of the benzene oxidation pathways at high concentrations of NO_x, above 5×10^{12} molecules cm^{-3}.[11,14] Furthermore, high concentrations of H atoms and O_2 can lead to the presence of HO_2 in the system that can react with OH aromatic adduct to introduce further loss of phenol in the system, as pointed out in Volkamer et al.[14] The large scale simulation chamber data sets are derived at much lower radical levels; hence the results obtained from the chamber studies are considered to be more atmospherically relevant. Our results demonstrate that the experimental conditions employed in this work give phenol yields that are compatible with those derived under atmospherically relevant conditions.

High radical concentrations have also been suggested to be at the core of apparent contradictory findings with regard to the presence of hexadienedials among first-generation oxidation products from the benzene + OH reaction. In the presence of moderately low concentrations of NO_x, hexadienedials were observed in a flow system,[16] but not observed in simulation chambers.[11,14] In this work we observed the presence of small amounts of 111 *m/z* in the benzene system, which could indicate formation of hexadienedials or catechols (indistinguishable in our CIMS analysis). The signal accounts for 10−15% of that of phenol. Part of that signal is due to catechol, which forms in high yields as a product of the OH radical reaction of phenol.[29] Phenol loss due to the OH reaction accounts for up to 5% correction on the measured amounts of phenol. If our setup was more sensitive to catechol than to phenol, then catechol could explain most of the 111 *m/z* signal, but some formation of hexadienedials cannot be ruled out completely. It is presently not clear whether radical−radical reactions or energy transfer from excited radicals formed in the initial stages of aromatic oxidation are at the core of the systematic differences found in previous flowtube studies and simulation chambers. Such reactions are systematically minimized in our study and do not appear to significantly affect the phenol yields obtained here.

Time Scale of Phenol Formation. We find that the phenol yield does not depend on the reaction time range examined and thus infer an upper limit time scale of phenol formation of 15 ms. Further, recent evidence from Master Equation calculations quantitatively reproduce this high phenol yield.[30] Figure 5 from Glowacki et al.[30] estimates the time scale of phenol formation from benzene to be 5−10 ms at 298 K, in good agreement with our upper limit of 15 ms. It is noteworthy that the high phenol yield is also broadly consistent with OH-cycling experiments, which find a 50% yield for "prompt" HO_2 formation from the benzene + OH reaction.[27] Within the error limits, all "prompt" HO_2 can be accounted for if its coproduct is phenol. Our results present the most direct evidence to date that phenol and HO_2 are quantitative coproducts of the same reaction channel. However, the results do not allow us to distinguish whether phenol is formed from the reaction of oxygen with the aromatic OH adduct or as a result of isomerization and subsequent decomposition of the aromatic−OH−O_2 adduct, though experimental[14] and theoretical[30] evidence points to the former pathway as being more relevant.

Toluene System: Cresol Yields. Table 2 shows the yield from the toluene + OH reaction. The cresol yield determined in this study 17.7 ± 2.1% is in excellent agreement with previous findings, which are 17.9 ± 2.7 and 17.9 ± 1.3% by Klotz et al.[18] and Smith et al.,[6] respectively. This is consistent with alkylbenzenes having a shorter lifetime during the initial equilibrium stages of aromatic oxidation[26,27,31] making toluene slightly less sensitive to interfering reactions from high radical concentrations than benzene.

TABLE 2: Selected Products of the Toluene + OH System

	% yield			
experiment OH + toluene	(cresols)[a]	(phenol)	time scale	setup (NO or NO_2 in ppm)
this work	17.7 ± 2.1	5.4 ± 1.2	~50 ms	flowtube (NO_x 0.01−0.1)
Klotz et al.[18]	17.9 ± 2.7	n.a.	5 min to 2 h	chamber low NO_x)
Smith et al.[6]	17.9 ± 1.3	<0.1	2 min	dynamic reactor (low NO_x)

[a] Combine d*o*-, *m*-, *p*-cresol.

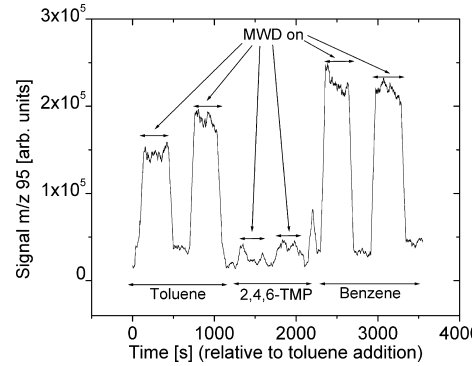

Figure 8. Direct evidence for dealkylation from toluene: Formation of *m/z* 95 from toluene and benzene under comparable FT conditions.

Dealkylation from the Toluene + OH Reaction. Surprisingly, the formation of a product with an *m/z* matching phenol·H^+ (*m/z* = 95) was observed. Figure 8 illustrates the formation of *m/z* 95 from toluene and benzene + OH in a separate sequence of experiments. First, only H atoms, NO_2, and the bath gas were introduced to the FT with MWD cycled between on and off to verify the cleanness of the system. There was no sign of *m/z* 95 formation with OH radicals present (not shown). Toluene was introduced at two different concentrations, ca. 2.7 and 4.2×10^{12} molecules cm^{-3}, and *m/z* 95 formation was observed. Then only ca. 9×10^9 molecules cm^{-3} of 2,4,6-TMP tracer was added to rule out the possibility of *m/z* 95 formation from the tracer; virtually no signal was observed. Finally in the absence of the tracer, only benzene was added to positively confirm the detection of phenol at *m/z* 95. The MWD was turned on and off twice for each compound to observe the *m/z* 95 signal and background in the absence of OH radicals. The *m/z* 95 signal was calibrated by flowing authentic phenol samples (see above), and yield numbers are given as "phenol equivalent" yields; however we note that benzene oxide/oxepin and phenol have identical molar masses and are expected to yield indistinguishable signals in our CIMS analysis. Similar amounts of *m/z* 95 are formed from benzene and toluene in these experiments. However, if the difference in reactivity between benzene and toluene is accounted for, the phenol equivalent yield from toluene is significantly lower.

The formation of m/z 95 from the toluene + OH reaction is surprising, as it requires loss of an alkyl substituent group from the benzene ring. Interestingly, Smith et al.[6] and Etzkorn[32] did observe phenol among the reaction products in small yields (<1%). In this work the contamination of the toluene bulb with benzene was negated by the absence of benzene signal with UV spectroscopy, consecutive experiments with only toluene, OH only background tests, and only benzene in the FT. Our

TABLE 3: Selected Products of the Xylenes + OH System

	% yield			
experiment	DMP	cresol	time scale	setup NO or NO_2 (in ppm)
OH + *m*-xylene	(2,4+2,6+3,5)			
DMP yield[f]	14.1 ± 2.6[a]			
this work		11.2 ± 3.8	~50 ms	flowtube NO_x 0.01−0.1
Atkinson et al.[34]	21.0 ± 5.6	n.a.	n.a.	chamber NO_2 0−10
Gery et al.[33]	17.8 ± 6.5	n.a.	8−23 min.	chamber NO_x 7.9−8.2
Smith et al.[5]	10.9 ± 0.5	n.a.	n.a.	dynamic reactor low NO_x
Zhao et al.[35]	17.3 ± 2.5[b]	n.a.	~50 ms	flowtube NO_2 20−45 ppb
OH + *o*-xylene	(2,3+3,4)			
DMP yield[f]	10.6 ± 4.7[c]			
this work		4.5 ± 3.2	~50 ms	flowtube NO_x 0.01−0.1
Atkinson et al.[34]	10.9 ± 2.6[d]	n.a.	n.a.	chamber NO_2 1−13
Gery et al.[33]	10.2 ± 3.9	n.a.	8−23 min.	chamber NO_x 8.0−8.2
OH + *p*-xylene	(2,5)			
DMP yield[f]	12.9 ± 2.9[e]			
this work		4.3 ± 3.1	~50 ms	flowtube NO_x 0.01−0.1
Atkinson et al.[34]	18.8 ± 3.8	n.a.	n.a.	chamber NO_2 1−10
Bethel et al.[36]	13.8 ± 1.6	n.a.	n.a.	chamber NO_2 0.8−3.3
Smith et al.[5]	13.0 ± 1.8	n.a.	n.a.	dynamic reactor low NO_x
Volkamer et al.[24]	11.9 ± 1.7	n.a.	5 min−2 h	chamber NO_x 0.5−600 ppb

[a] The DMP reference yield represents the average from Smith et al.[5] and Zhao et al.[35] [b] Sum of 2,4- and 2,6-DMP. [c] The DMP reference yield represents the average from Atkinson et al.[34] and Gery et al.[33] [d] DMP yield is scaled from low NO_x experiments in *p*- and *m*-xylene. n.a., not available. [e] The DMP reference yield represents the average from Smith et al.,[5] Bethel et al.,[36] and Volkamer et al.[24] [f] Yield used as reference in the relative determination of the cresol equivalent yield.

findings present the first systematic study to yield direct evidence that "dealkylation" presents a viable and an active pathway for toluene.

Dealkylation from the Xylene + OH Systems. Furthermore, products from the series of *o*-, *m*-, and *p*-xylene were investigated. Table 3 indicates the formation of dimethylphenol (DMP, *m*/*z* 123) and products with *m*/*z* 109 (equivalent mass of cresol in our CIMS). For these compounds, the 2,4,6-TMP tracer interfered with the signal at *m*/*z* 137, which was also generated from the reaction of xylene and OH radicals. Instead, experiments were conducted in the absence of any tracer, and the relative yield method was employed: DMP yields from the literature[6,14,24,33−36] were used as reference yields to estimate cresol equivalent yields using eq 5:

$$\text{yield} = \frac{m/z\ 109\ \text{signal}}{m/z\ 123\ \text{signal}} \times \text{yield of DMP literature average} \quad (5)$$

The reference DMP yields are obtained from the selected literature values as listed in Table 3. Only one study is available that quantifies a DMP yield for the *o*-xylene under high NO_x concentrations.[34] The DMP yield values from Atkinson et al.[34] showed consistently greater values than the other studies for all three xylene isomers; therefore, the sum of DMP for *o*-xylene was scaled down from 16.1 ± 2.8% to 10.9 ± 2.6%, reflecting

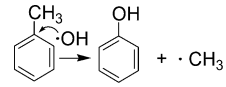

Figure 9. Phenol formation from toluene via addition of OH in the ipso position.

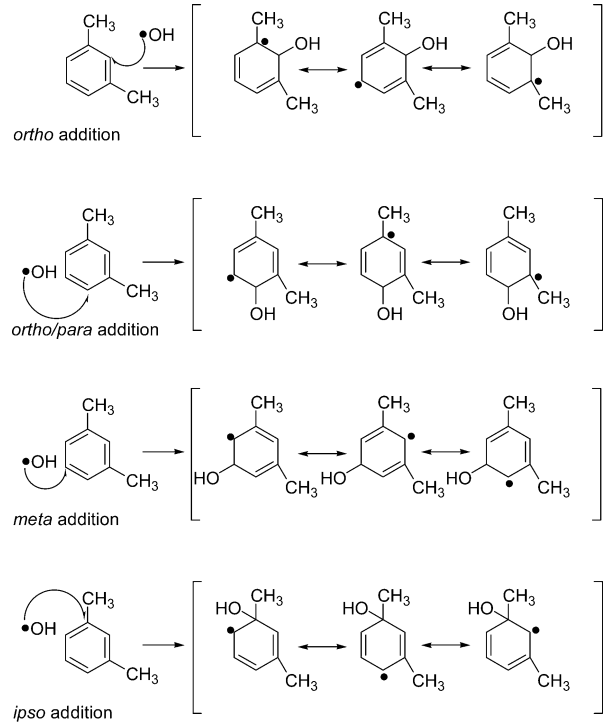

Figure 10. Resonance structures for the OH addition reaction to *m*-xylene.

the effect of high NO_x on DMP yields for other xylene isomers, where yields that do not suffer apparent NO_x effects are available.

Among the three isomers, *m*-xylene showed the greatest cresol equivalent yield of 11.2 ± 3.8%, while the *o*- and *p*-xylene showed 4.5 ± 3.2% and 4.3 ± 3.1%, respectively. The large relative errors for the *p*- and *o*-xylenes are introduced from the reference data errors as shown in Table 3. The isomer effect for higher dealkylation from *m*-xylene is highly significant, and beyond experimental uncertainty.

Semiquantitative Explanation for the Isomer Effect of Dealkylation. To the best of our knowledge, this is the first evidence for dealkylation from the *o*-, *m*-, and *p*-xylene systems reported to date. There are two possible pathways that could explain our results. One possibility for a reaction mechanism could involve the addition of the OH radical in the ipso position (in analogy to Figure 9). Recently Bohn et al.[37] and Koch et al.[38] presented indirect experimental evidence that suggests the ipso addition of OH contributes to OH decays for the trimethylbenzene (TMB) + OH reaction. Furthermore, the ipso addition of OH + hexamethylbenzene (HMB) was inferred from the observation of a higher rate constant than the expected H-abstraction alone.[17] A direct experimental observation of the ipso addition pathway is yet to be accomplished. The use of deuterated aromatics in OH-cycling experiments has some potential to shed more light on the role of the ipso channel.[37,38] A theoretical study using density function theory (DFT) to study the *p*-xylene + OH reaction[39] predicted OH radical addition to proceed with a 20% probability in the ipso position. Suh et al.[40] estimates a net 3% of ipso addition from their theoretical work for the *m*-xylene + OH system. The role of the ipso-addition

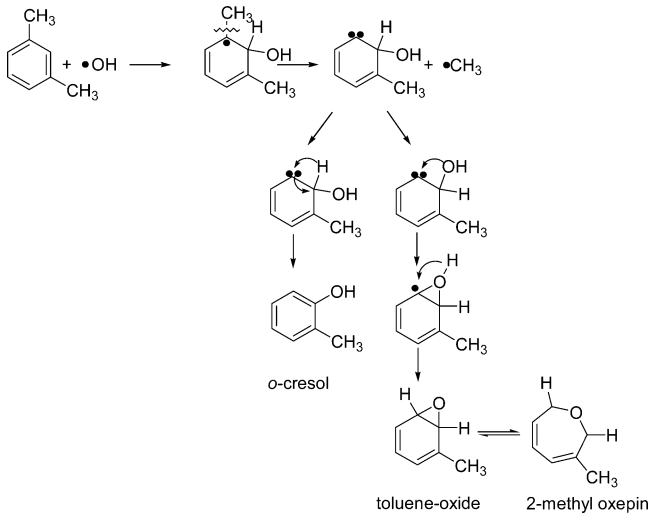

Figure 11. Proposed pathway leading to the formation of *o*-cresol and epoxide-type products with the same *m*/*z* from *m*-xylene.

pathway in dealkylation remains to be determined. Existing evidence is inconclusive as to the relevance of this pathway; for *m*-xylene the yield appears to be too low to explain the observed cresol equivalent signal by ipso addition alone in this study. Further, any isomer effect is not expected. An alternative mechanism for dealkylation appears to be needed to explain the isomer effect observed for xylenes. An alternative mechanism that can explain the isomer effect is presented in Figures 10 and 11. Notably, the OH radical adds preferentially in the ortho position to alkyl-substituent groups. For OH-adducts in the ortho and para positions, the unpaired electron is resonance-stabilized at a methyl-substituted carbon of the ring system. Figure 10 illustrates the possible resonance structures for OH-addition to *m*-xylene; following addition in the ortho position the unpaired radical is located for two out of three possible resonance structures at the methyl-substituted carbon. Table 4 further extends this idea, making use of experimental and computational evidence for the relative probabilities for the OH radical to add to different positions of the aromatic ring. When this probability for initial OH-radical attack is multiplied by the probability for resonance stabilization of the radical at a methyl-substituted carbon, the relative probability for unpaired electrons to be located at alkyl-substituted groups is about two times higher for *m*-xylene (194%) than for toluene, *o*-xylene, or *p*-xylene (86−100%). This difference agrees remarkably well with the about twice higher yields for dealkylation from *m*-xylene compared to toluene and *o*- and *p*-xylene. The particularly efficient dealkylation of *m*-xylene upon OH oxidation hence is tentatively assigned to two factors: (1) a high probability for OH to add in the ortho position, 97%,[5] and (2) the high probability of having the unpaired radical at a methyl-substituted carbon. Figure 11 illustrates the formation of cresol and toluene 1,2-oxide and 2-methyloxepin from xylene via carbene-type intermediates. Similarly, benzene oxide/oxepin could form in addition to phenol from toluene. Notably, toluene 1,2-oxide/2-methyloxepin or benzene oxide/oxepin have the same sum formulas as cresol (C_7H_8O) or phenol (C_6H_6O) and—if formed—are expected to contribute efficiently to the signal at *m*/*z* 109 or *m*/*z* 95 in our CIMS analysis. Useful information to distinguish these products can be obtained by means of GC/MS and/or FTIR in future studies.[16,41] The lack of authentic standards for epoxides complicates the quantification of the overall yield of dealkylation but does not affect our conclusion that dealkylation is operative. Dealkylation yields are quantified here as phenol and cresol equivalent yields from toluene and xylenes assuming an equal sensitivity to the phenol- and/or epoxide-type compounds. Notably, the isomer effect is identified here only from a relative comparison of yield numbers; any uncertainties in the absolute yield numbers hence do not affect the implications for the reaction mechanism of dealkylation.

The radical-type intermediates, i.e., OH adducts and subsequent peroxy radicals carry excess energies of 10−40 kcal/mol,[40,42] which is lower than the C−C bond energy of 103 kcal/mol.[43] Currently there is no theoretical study of the C−C bond energy of an alkyl-substituted aromatic ring carbon activated by an unpaired electron. Further, studies of the decomposition of alkoxy radicals show that the activation energy for decomposition via C−C bond cleavage depends on the alkyl substituents: for example the barrier for elimination lowers as the alkyl chain increases in length.[44,45] In analogy, if the alkyl radicals formed upon OH-addition to alkylbenzenes followed this tendency observed for alkoxy radicals, alkylbenzenes with longer side chains (i.e., ethylbenzene, *m*-ethyltoluene, *tert*-butylbenzene,

TABLE 4: Explanation of the Isomer Effect for m-Xylene in Terms of Resonance Stabilization of the Delocalized Electron of the OH-Adduct to be Located at a Methyl-Substituted Ring Carbon: Correspondence of Relative Probabilities and Yields

		OH addition branching ratio		resonance probability		
compound	position	theoretical (%)	experimental (%)	weight *x*/3	overall probability[h]	yield (%) this work
toluene	ortho	48[a]	68[b]	1		phenol
	meta	15[a]	16[b]	0	0.86(0.74)	5.4 ± 1.2
	para	26[a]	16[b]	1		
	ipso	8[a]	n.a.	0		
m-xylene	ortho	97[c]	97[d]	2		cresol
	meta	2[c]	3[d]	0	1.94(1.94)	11.2 ± 3.8
	ipso	1[c]	n.a.	0		
o-xylene	ortho	n.a.	60[e]	1		cresol
	meta/para	n.a.	40[e]	1	1.0(1.0)	4.5 ± 3.2
	ipso	∼20[f]	n.a.	1		
p-xylene	ortho	80[g]	100	1		cresol
	ipso	20[g]	n.a.	1	1.0(1.0)	4.3 ± 3.1

[a] Average data from Suh et al.[40] and Uc et al.[50] [b] Average data from Smith et al.[6] and Klotz et al.[18] [c] Fan and Zhang.[51] [d] Smith et al.[5] [e] Atkinson et al.[34] [f] Approximated based on Fan and Zhang[39] and Huang et al.[52] [g] Fan and Zhang.[39] [h] Overall probability for resonance stabilization calculated as the sum over OH-addition positions, of the OH-addition branching ratio multiplied by the statistical "weight" of resonance stabilization (illustrated in Figure 10). Values in parentheses indicate numbers based on theory (note that weights for *o*- and *p*-xylene are equal for all positions of OH attack, and hence the overall probability is 1, independent of the position of initial OH-radical attack).

etc.) would show a similar or higher probability for dealkylation than toluene and the xylenes. It would be worthwhile to investigate the decomposition pathways of OH adducts also from other alkylbenzenes, such as 1,3,5-TMB and HMB.

Dependence of the Dealkylation Pathway on Experimental Conditions. Notably, special care was taken in this study to conduct experiments at atmospherically relevant oxygen concentrations. Most experiments were conducted at 150 Torr of O_2 partial pressure to ensure that the initial equilibrium stages of sequential O_2 addition to the OH adduct, as well as the fate of the peroxy-bridged radical, closely resemble that under atmospheric conditions. Notably, the phenol yield from benzene and the cresol yield from toluene determined at 154 Torr total pressure in this work agree well with yields from chambers at 760 Torr and comparable oxygen concentration.[6,14,18] This absence of a pressure dependence is consistent with early work by Atkinson et al.,[46] who found *o*-cresol yields from toluene to be constant over 62−740 Torr. However they identified a slight pressure effect for ring-cleavage products (25% lower biacetyl yields from *o*-xylene at lower pressure). Recent theoretical evidence demonstrates for benzene that the rates of reaction at 150 Torr differ from those at 760 Torr by a factor of 1.4 to 2;[30] the study further suggests a pressure dependence for epoxide formation. Notably, the mechanism of epoxide formation proposed here is different from previously studied pathways.[30,41,47,48] Significant phenol yields from toluene are observed also at 760 Torr total pressure;[6,32] those yields increase with increasing oxidation times: yields <0.1% are observed after a few minutes of oxidation;[6] phenol yields increased from virtually zero after a few tens of minutes of oxidation to values of up to 1% after several hours at EUPHORE.[32] Notably, the thermal decomposition and photolysis reactions of benzene oxide/oxepin efficiently form phenol as the major product (53% yield from photolysis);[53] increasing phenol yields with time indicate that phenol forms as a second or higher generation product from toluene, compatible with epoxide-type products as intermediates. In combination with the dealkylation isomer effect this suggests that the major products of the dealkylation pathway identified in this study are epoxide-type products, with phenol-type products making a minor (possibly negligible) contribution. Assuming that all phenol forms from toluene via benzene oxide/oxepin photolysis at EUPHORE,[32] and assuming further that the benzene oxide/oxepin loss is equally determined by photolysis and OH-radical reaction (only the former forms phenol),[53] a phenol yield of 1% corresponds to 3.8% dealkylation yield from toluene. This suggests a minor pressure effect (similar to that found in ref 46); the agreement between dealkylation yields inferred at 760 Torr and yields measured at 154 Torr is remarkable. Dealkylation appears to be a significant pathway also at atmospheric pressure. Such good agreement suggests that the effect of pressure on the dealkylation pathway—though not implausible—is unlikely to change our conclusions that dealkylation is operative also at atmospheric pressure.

Conclusions

A flowtube study with a series of monocyclic compounds (benzene, toluene, *o*-, *m*-, and *p*-xylene) reacting with OH radicals showed evidence for dealkylation to form phenol-type and likely epoxide-type products. Surprisingly, at 154 Torr the dealkylation of toluene proceeds at yields that are equivalent to 5.4 ± 1.2% phenol; similarly, dealkylation from *m*-, *o*-, and *p*-xylene proceeds at yields that are equivalent to 11.2 ± 3.8%, 4.5 ± 3.2%, and 4.3 ± 3.1% cresol, respectively. A significant isomer effect is observed for *m*-xylene. Two alternative pathways for dealkylation are proposed, which are initiated by (1) ipso addition of OH or (2) ortho/para addition of OH, and both result in activation of the methyl-substituted ring carbon. While our CIMS analysis does not distinguish between these pathways, only the second mechanism can explain the isomer effect among xylenes.

Dealkylation may be a general pathway in aromatic oxidation and should be considered in future experimental and theoretical studies. A pressure-dependent study of dealkylation using a combination of techniques to detect multiple products, including isomer-specific analytical tools, holds great promise to obtain further insights in the dealkylation mechanism, and its atmospheric relevance. If dealkylation was confirmed to be a general pathway also from other aromatic species, it would help to improve the poor carbon balance of identified products typical for aromatic oxidation and would likely add valuable information about structure−activity relations in the early stages of aromatic oxidation. Among the products from the dealkylation, the alkyl groups (methyl radicals) are a source of RO_2 radicals that propagate either to form methyl peroxide or to form formaldehyde and HO_2 radicals; longer chain alkyl groups could be a source for longer chain aldehydes and hydroperoxides. Aldehydes and hydroperoxides upon their photolysis add a radical source in the urban and remote atmosphere. Epoxides are a potential concern for public health.

Acknowledgment. This work was funded by the U.S. Department of Energy. The authors acknowledge L. Shaw and K. Boyle for providing access to their respective UV spectrometers at MIT CMSE and the Anderson lab at Scripps Institution of Oceanography and T. Sammakia and B. Ellison for helpful discussions. J.N. acknowledges a fellowship by the Knut and Allice Wallenbergs foundation. R.V. acknowledges consecutive fellowships by the Henry & Camille Dreyfus Foundation and the Alexander von Humboldt Foundation.

References and Notes

(1) United Nations Development programme *World population prospects: The 2002 revision and world urbanization prospects*; U.N. secretary: New York, 2005,

(2) Kurtenbach, R.; Ackermann, R.; Becker, K. H.; Geyer, A.; Gomes, J. A. G.; Lorzer, J. C.; Platt, U.; Wiesen, P. *J. Atmos. Chem.* **2002**, *42* (1), 395–411.

(3) Velasco, E.; Lamb, B.; Westberg, H.; Allwine, E.; Sosa, G.; Arriaga-Colina, J. L.; Jobson, B. T.; Alexander, M. L.; Prazeller, P.; Knighton, W. B.; Rogers, T. M.; Grutter, M.; Herndon, S. C.; Kolb, C. E.; Zavala, M.; de Foy, B.; Volkamer, R.; Molina, L. T.; Molina, M. J. *Atmos. Chem. Phys.* **2007**, *7*, 329–353.

(4) Calvert, J. G., Atkinson, R., Becker, K. H., Kames, R. M., Seinfeld, J. H., Wallington, T. J., Yarwood, G., *The Mechanisms of Atmospheric Oxidation of Aromatic Hydrocarbons*; Oxford Universtiy Press: New York, 2002.

(5) Smith, D. F.; Kleindienst, T. E.; McIver, C. D. *J. Atmos. Chem.* **1999**, *34* (3), 339–364.

(6) Smith, D. F.; McIver, C. D.; Kleindienst, T. E. *J. Atmos. Chem.* **1998**, *30* (2), 209–228.

(7) Volkamer, R.; Spietz, P.; Burrows, J.; Platt, U. *J. Photochem. Photobiol., A* **2005**, *172* (1), 35–46.

(8) Volkamer, R.; Jimenez, J. L.; San Martini, F.; Dzepina, K.; Zhang, Q.; Salcedo, D.; Molina, L. T.; Worsnop, D. R.; Molina, M. J. *Geophys. Res. Lett.* **2006**, *33* (17), 4.

(9) Sheehy, P. M.; Volkamer, R.; Molina, L. T.; Molina, M. J. *Atmos. Chem. Phys. Discuss.* **2008**, *8*, 5359–5412.

(10) Atkinson, R.; Arey, J. *Chem. Rev.* **2003**, *103* (12), 4605–4638.

(11) Klotz, B.; Volkamer, R.; Hurley, M. D.; Andersen, M. P. S.; Nielsen, O. J.; Barnes, I.; Imamura, T.; Wirtz, K.; Becker, K. H.; Platt, U.; Wallington, T. J.; Washida, N. *Phys. Chem. Chem. Phys.* **2002**, *4* (18), 4399–4411.

(12) Volkamer, R.; Uecker, J.; Wirtz, K.; Platt, U. OH-Radical initiated Oxidation of BTXM: Formation and Atmospheric Fate of Phenol-type compounds in the Presence of NOx. In *EUROTRAC-2 Symposium 2002,*

Transport and Chemical Transformation in the Troposphere; Margraf Verlag, Weikersheim: Garmisch-Partenkirchen, Germany, 2002.

(13) Atkinson, R.; Aschmann, S. M. *Int. J. Chem. Kinet.* **1994**, *26* (9), 929–944.

(14) Volkamer, R.; Klotz, B.; Barnes, I.; Imamura, T.; Wirtz, K.; Washida, N.; Becker, K. H.; Platt, U. *Phys. Chem. Chem. Phys.* **2002b**, *4* (9), 1598–1610.

(15) Berndt, T.; Boge, O. *Phys. Chem. Chem. Phys.* **2006**, *8* (10), 1205–1214.

(16) Berndt, T.; Boge, O.; Herrmann, H. *Chem. Phys. Lett.* **1999**, *314* (5−6), 435–442.

(17) Berndt, T.; Boge, O. *Phys. Chem. Chem. Phys.* **2001**, *3* (22), 4946–4956.

(18) Klotz, B.; Sorensen, S.; Barnes, I.; Becker, K. H.; Etzkorn, T.; Volkamer, R.; Platt, U.; Wirtz, K.; Martin-Reviejo, M. *J. Phys. Chem. A* **1998**, *102* (50), 10289–10299.

(19) Molina, M. J.; Zhang, R.; Broekhuizen, K.; Lei, W.; Navarro, R.; Molina, L. T. *J. Am. Chem. Soc.* **1999**, *121* (43), 10225–10226.

(20) Lipson, J. B.; Elrod, M. J.; Beiderhase, T. W.; Molina, L. T.; Molina, M. J. *J. Chem. Soc., Faraday Trans.* **1997**, *93* (16), 2665–2673.

(21) Stutz, J.; Platt, U. *Appl. Opt.* **1996**, *35* (30), 6041–6053.

(22) Fayt, C. a.v. R. *M. WinDoas 2.1 - Software User Manual*; BIRA-IASB: Brussels, 2001.

(23) *CRC handbook of chemistry and physics: a ready-reference book of chemical and physical data*; Lide, D. R., Ed.; CRC Press: Boca Raton, FL, 2004.

(24) Volkamer, R. A DOAS study on the Oxidation Mechanism of Aromatic Hydrocarbons under Simulated Atmospheric Conditions. Ph.D. Thesis, Rupertus Carola University of Heidelberg, Heidelberg, Germany, 2001.

(25) Bloss, C.; Wagner, V.; Jenkin, M. E.; Volkamer, R.; Bloss, W. J.; Lee, J. D.; Heard, D. E.; Wirtz, K.; Martin-Reviejo, M.; Rea, G.; Wenger, J. C.; Pilling, M. J. *Atmos. Chem. Phys.* **2005**, *5*, 641–664.

(26) Bohn, B. *J. Phys. Chem. A* **2001**, *105* (25), 6092–6101.

(27) Bohn, B.; Zetzsch, C. *Phys. Chem. Chem. Phys.* **1999**, *1* (22), 5097–5107.

(28) Atkinson, R.; Aschmann, S. M.; Arey, J.; Carter, W. P. L. *Int. J. Chem. Kinet.* **1989**, *21* (9), 801–827.

(29) Olariu, R. I.; Klotz, B.; Barnes, I.; Becker, K. H.; Mocanu, R. *Atmos. Environ.* **2002**, *36* (22), 3685–3697.

(30) Glowacki, D. R. W., L.; Pilling, M. J. , J. Phys. Chem. A, Submitted for publication.

(31) Raoult, S.; Rayez, M. T.; Rayez, J. C.; Lesclaux, R. *Phys. Chem. Chem. Phys.* **2004**, *6* (9), 2245–2253.

(32) Etzkorn, T., *Personal communication*, Heidelberg, Germany, 2000.

(33) Gery, M. W.; Fox, D. L.; Kamens, R. M.; Stockburger, L. *Environ. Sci. Technol.* **1987**, *21* (4), 339–348.

(34) Atkinson, R.; Aschmann, S. M.; Arey, J. *Int. J. Chem. Kinet.* **1991**, *23* (1), 77–97.

(35) Zhao, J.; Zhang, R. Y.; Misawa, K.; Shibuya, K. *J. Photochem. Photobiol., A* **2005**, *176* (1−3), 199–207.

(36) Bethel, H. L.; Atkinson, R.; Arey, J. *J. Phys. Chem. A* **2000**, *104* (39), 8922–8929.

(37) Bohn, B., Elend, M.; Zetzsch, C. *Abbaumechansmne von Aromaten nach Anlagerung von OH und ihr Einfluss auf die Kreisälufe von HOx unter Bildung von Photoxidantien*; **2000**; pp 217−227.

(38) Koch, R.; Knispel, R.; Elend, M.; Siese, M.; Zetzsch, C. *Atmos. Chem. Phys.* **2007**, *7* (8), 2057–2071.

(39) Fan, J. W.; Zhang, R. Y. *J. Phys. Chem. A* **2006**, *110* (24), 7728–7737.

(40) Suh, I.; Zhang, D.; Zhang, R. Y.; Molina, L. T.; Molina, M. J. *Chem. Phys. Lett.* **2002**, *364* (5−6), 454–462.

(41) Klotz, B.; Barnes, I.; Becker, K. H. *Chem. Phys.* **1998**, *231* (2−3), 289–301.

(42) Lay, T. H.; Bozzelli, J. W.; Seinfeld, J. H. *J. Phys. Chem.* **1996**, *100* (16), 6543–6554.

(43) Blanksby, S. J.; Ellison, G. B. *Acc. Chem. Res.* **2003**, *36* (4), 255–263.

(44) Atkinson, R. *Int. J. Chem. Kinet.* **1997**, *29* (2), 99–111.

(45) Atkinson, R. *Atmos. Environ.* **2007**, *41* (38), 8468–8485.

(46) Atkinson, R.; Carter, W. P. L.; Winer, A. M. *J. Phys. Chem.* **1983**, *87* (9), 1605–1610.

(47) Baltaretu, C. O.; Lichtman, E. I.; Hadler, A. B.; Elrod, M. J. *J. Phys. Chem. A* **2009**, *113* (1), 221–230.

(48) Yu, J. Z.; Jeffries, H. E. *Atmos. Environ.* **1997**, *31* (15), 2281–2287.

(49) Bjergbakke, E.; Sillesen, A.; Pagsberg, P. *J. Phys. Chem.* **1996**, *100* (14), 5729–5736.

(50) Uc, V. H.; Alvarez-Idaboy, J. R.; Galano, A.; Vivier-Bunge, A. *J. Phys. Chem. A* **2008**, *112* (33), 7608–7615.

(51) Fan, J. W.; Zhang, R. Y. *J. Phys. Chem. A* **2008**, *112* (18), 4314–4323.

(52) Huang, M. Q.; Zhang, W. J.; Wang, Z. Y.; Hao, L. Q.; Zhao, W. W.; Liu, X. Y.; Long, B.; Fang, L. *Int. J. Quantum Chem.* **2008**, *108* (5), 954–966.

(53) Klotz, B.; Barnes, I.; Becker, K. H.; Golding, B. T. *J. Chem. Soc., Faraday Trans.* **1997**, *93*, 1507.

JP901529K